Identification of Insulin-Responsive Transcription Factors That Regulate Glucose Production by Hepatocytes

Liheng Wang,[1,2] Qiongming Liu,[3] Takumi Kitamoto,[1,2] Junjie Hou,[4] Jun Qin,[3] and Domenico Accili[1,2]

Diabetes 2019;68:1156–1167 | https://doi.org/10.2337/db18-1236

Hepatocyte glucose production is a complex process that integrates cell-autonomous mechanisms with cellular signaling, enzyme activity modulation, and gene transcription. Transcriptional mechanisms controlling glucose production are redundant and involve nuclear hormone receptors and unliganded transcription factors (TFs). Our knowledge of this circuitry is incomplete. Here we used DNA affinity purification followed by mass spectrometry to probe the network of hormone-regulated TFs by using phosphoenolpyruvate carboxykinase (*Pck1*) and glucose-6-phosphatase (*G6pc*) in liver and primary hepatocytes as model systems. The repertoire of insulin-regulated TFs is unexpectedly broad and diverse. Whereas in liver the two test promoters are regulated by largely overlapping sets of TFs, in primary hepatocytes *Pck1* and *G6pc* regulation diverges. Insulin treatment preferentially results in increased occupancy by the two promoters, consistent with a model in which the hormone's primary role is to recruit corepressors rather than to clear activators. Nine insulin-responsive TFs are present in both models, but only FoxK1, FoxA2, ZFP91, and ZHX3 require an intact *Pck1p* insulin response sequence for binding. Knockdown of FoxK1 in primary hepatocytes decreased both glucose production and insulin's ability to suppress it. The findings expand the repertoire of insulin-dependent TFs and identify FoxK1 as a contributor to insulin signaling.

The liver produces glucose during fasting in order to maintain euglycemia. This process becomes altered in diabetes, when resistance to or a lack of insulin increases glucose production, contributing to hyperglycemia and its complications (1). Hepatocyte glucose production is a complex, multilayered process that involves contributions from other organs in the form of glucogenic substrates, and an intracellular shift of the glucose-6-phosphate pool from use via glycolysis or glycogen-triglyceride synthesis to dephosphorylation and release as glucose (2). The latter process integrates cellular signaling, enzyme activity modulation, and gene transcription (1).

Transcriptional mechanisms controlling glucose production are famously redundant, with nuclear hormone receptors and posttranslationally modified transcription factors (TFs) without ligands participating in the process (3–5). But loss-of-function experiments in mice have shown that many genes continue to be properly regulated in the absence of these factors, indicating that our knowledge of the circuitry is incomplete (5–8). An interesting example of this partial knowledge is a comparison of two genes of historical interest in hormone action research: glucose-6-phosphatase (*G6pc*) and phosphoenolpyruvate carboxykinase (*Pck1*). Irrespective of their actual contributions to hepatic glucose production, these two genes are useful as a model for understanding how the two competing branches of glucose metabolism—the anabolic insulin-dependent branch and the catabolic glucagon/glucocorticoid-dependent branch—act transcriptionally. *Pck1* and *G6pc* share transcriptional regulators such as glucocorticoid receptor (GR), FoxO1, CREBP, CRCT2, and C/EBPα/β (4,5,9–12). However, they respond differently to these TFs. Thus, when FoxO is ablated, hormonal modulation of *G6pc* is completely abolished while regulation of *Pck1* is largely retained (5,7,13). These findings highlight a gap in our knowledge of the broader set of TFs

[1]Department of Medicine, Vagelos College of Physicians and Surgeons, Columbia University, New York, NY
[2]Naomi Berrie Diabetes Center, Vagelos College of Physicians and Surgeons, Columbia University, New York, NY
[3]State Key Laboratory of Proteomics, Beijing Proteome Research Center, Beijing Institute of Lifeomics, National Center for Protein Sciences, Beijing, China
[4]National Laboratory of Biomacromolecules, Chinese Academy of Sciences Center for Excellence in Biomacromolecules, Institute of Biophysics, Chinese Academy of Sciences, Beijing, China

Corresponding author: Domenico Accili, da230@cumc.columbia.edu

Received 20 November 2018 and accepted 20 March 2019

This article contains Supplementary Data online at http://diabetes.diabetesjournals.org/lookup/suppl/doi:10.2337/db18-1236/-/DC1.

acting on these promoters that can account for the complexity of the hormonal response to nutrients.

DNA affinity purification coupled with mass spectrometry (MS) has been used to identify TFs and chromatin-bound complexes required for gene regulation (14). Here we used it to probe the network of hormone-regulated TFs, with *Pck1* and *G6pc* promoters (*Pck1p* and *G6pcp*) in whole liver and primary hepatocytes as the targets, and to unravel their unexpectedly vast repertoire.

RESEARCH DESIGN AND METHODS

Study Design

To identify the network of TFs regulating expression of the gluconeogenic genes *Pck1* and *G6pc*, we combined DNA affinity pull down and MS analysis. In the DNA pull-down experiments, we used nuclear proteins isolated from liver from mice that were deprived of food (for 16 h overnight) and mice that were refed (deprived of food for 16 h then refed over 4 h) or primary hepatocytes that received various hormone treatments. We sorted and analyzed TFs based on how they responded to refeeding, dexamethasone (Dex) and cAMP (D/C), and Dex, cAMP, and insulin (D/C/I). Comparison of the two promoters further defined common and selective insulin-regulated TFs. Comparison of in vivo and in vitro models identified conserved insulin-regulated TFs. To validate the findings, we performed functional studies of one selected candidate in whole liver and primary hepatocytes, demonstrating its role in modulating glucose production.

Primary Hepatocyte Studies

Primary hepatocytes were isolated from 8- to 12-week-old male C57/B6 or FoxO1 flox/flox mice, as described previously (15). All animal studies were approved by the Columbia Institutional Animal Care and Use Committee. Isolated primary hepatocytes were resuspended in hepatocyte plating medium (Medium 199 supplemented with 10% FBS [Thermo Fisher Scientific, Waltham, MA], 100 units/mL penicillin-streptomycin [Thermo Fisher Scientific], and 10 μg/mL gentamicin [Sigma-Aldrich, St. Louis, MO]), and 10^7 cells were placed in a 150-mm (in diameter) dish, or 5×10^5 cells were applied in each well of a 12-well collagen-coated plate. After culturing for 24 h, cells were incubated overnight in hepatocyte starvation medium comprising Medium 199 supplemented with 1% BSA (Sigma-Aldrich), penicillin-streptomycin, and gentamicin. Thereafter either the vehicle (0.002% methanol) or 1 μmol/L Dex and 0.1 mmol/L cAMP were added and left for 6 h. Then 100 nmol/L insulin was added and left for 30 min. Cells were then lysed in order to isolate protein.

Cells were ready 2 h after plating for siRNA transfection or adenovirus infection. Wild-type primary hepatocytes were transfected with control (AM4611) or Foxk1 siRNA mix (Thermo Fisher Scientific) using the Viromer BLUE transfection reagent (Lipocalyx, Halle, Germany). Foxk1 siRNA mix includes two siRNAs: FoxK1 silencer siRNA 67984 (sense) (GGAGCCUCACUUCUAUCUUtt) and siRNA2 68712 (sense) (GGGCUCUUUUUGGCGAAUAtt). FoxO1 flox primary hepatocytes were infected with adenovirus-Cre (Welgen, Worcester, MA) at 10 multiplicities of infection. After transfection (48 h), we replaced the medium with hepatocyte starvation medium, left it overnight, and then treated cells with D/C or D/C/I, as described above. Glucose production was assayed as previously described (15).

DNA Pull Down and Western Blotting

We amplified *Pck1p* (−600 to +69 base pairs [bp]) and *G6pcp* (−509 to +53 bp) from mouse genomic DNA using primers labeled with 5′-biotin: *Pck1p* forward, AGCTTACAGCCACTCCTAATCTCTG; *Pck1p* reverse, CAGAGATCGCTGAGCGCCTTG; *G6pcp* forward, ACGTGAACTTGGTGAAAGTCCA; *G6pcp* reverse, TACCTCAGGAAGCTGCCAGC. The *Pck1pΔIRS* promoter sequence (−600 to −417 bp, −401 to +69 bp) was amplified from the *Pck1pΔIRS*-MXS-mCherry plasmid by using the same biotin-labeled *Pck1p* primers. We cloned *Pck1p* into pMXS-mCherry through the use of In-Fusion Cloning with the following primers: *Pck1p*-MXS forward, TCAGTGAGCCATGATAGCTTACAGCCACTCCTAATCTCTG; *Pck1p*-MXS reverse: CATTCGAGTTACGCGGATCGCTGAGCGCCTTG. The pMXS-mCherry plasmid was linearized with *Eco*RV and MluI for In-Fusion recombination, followed by site-directed mutagenesis in order to generate the *Pck1pΔIRS*-MXS-mCherry plasmid by using two ΔIRS primers: forward, CAGCAGCCACCGGCACAC; reverse, CAGCTGTGAGGTGTCACTCCC. We sequenced each plasmid at Genewiz (South Plainfield, NJ) to confirm the mutation.

Biotinylated *Pck1p* or *G6pcp* fragments were immobilized on Dynabeads M-280 Streptavidin (Invitrogen, Carlsbad, CA) with DNA binding buffer (5 mmol/L Tris [pH 7.5], 0.5 mmol/L EDTA, 1 mol/L NaCl) and washed with BC-150 buffer (20 mmol/L Tris [pH 7.3], 150 mmol/L NaCl, 0.2 mmol/L EDTA, 20% glycerol). We prepared nuclear extracts using NE-PER Nuclear and Cytoplasmic Extraction Reagents containing Halt protease and a phosphatase inhibitor cocktail (Thermo Fisher Scientific). Before adding *Pck1p* Dynabeads, the nuclear extract was adjusted to 200–250 mmol/L total salt with BC-0 (20 mmol/L Tris [pH 7.3], 0.2 mmol/L EDTA, 20% glycerol) and 1 mmol/L EGTA/EDTA. *Pck1p* Dynabeads were incubated with rotation with 0.5 mg nuclear extract at 4°C overnight. The supernatant was discarded and the beads were washed twice with NETN buffer (50 mmol/L NaCl, 1 mmol/L EDTA, 20 mmol/L Tris [pH 8.0], 0.5% NP-40) and three times with PBS. Beads were resuspended in 50 μL sample buffer, boiled for 5 min, and fractionated on 10% SDS-PAGE. Gels were stained with EZBlue Gel Staining Reagent (Sigma-Aldrich). Half the volume of pull-down samples or 30 μg of raw protein lysate from each sample were used for Western blotting. Membranes were prestained with Ponceau Red solution (0.1% [w/v]) and cut into strips on the basis of molecular weight. Information about antibodies is in Supplementary Table 7.

Nano Liquid Chromatography/MS Analysis

Samples were analyzed with an Orbitrap Fusion mass spectrometer coupled with an Easy-nLC 1000 nanoflow liquid chromatography system (Thermo Fisher Scientific). The quantities of identified proteins were estimated by using the intensity-based absolute quantification (iBAQ) method. TFs were annotated from identified nuclear proteins according to the DBD database (16). We subtracted the iBAQ value of negative control samples from those of all treatment groups. ΔiBAQ <0 were assigned an arbitrary value of 0. We generated heat maps on the basis of a normalized iBAQ value by using One Matrix Clustered Image Maps (https://discover.nci.nih.gov/cimminer/oneMatrix.do). We analyzed functional annotation of TF lists and pathways of TFs by using the ConsensusPathDB gene set analysis tool (http://cpdb.molgen.mpg.de) for overrepresentation analysis. More details are available in the Supplementary Data.

RNA Isolation and Quantitative PCR Analysis

We lysed primary hepatocytes or liver in 1 mL TRIzol reagent. We purified RNA further using an RNeasy Mini Kit (Qiagen, Germantown, MD). For reverse transcription, we used a qScript cDNA Synthesis Kit (QuantaBio, Beverly, MA). RNA (1 μg) was used for each reverse transcriptase reaction. The 20 μL cDNA solution was diluted with RNase-free water to a final volume of 0.2 mL. We used GoTaq qPCR Master Mix (Promega, Madison, WI) for subsequent quantitative (q)PCR analysis. Primer information is available in Supplementary Table 8.

Luciferase Assay

pRL3 basic was linearized with *Kpn*I and *Hin*dIII, and promoter fragments were cloned with an In-Fusion cloning kit. Primers used for promoter amplification included the pGL3-*Pck1p* forward primer TTTCTCTATCGATAGAGCTTACAGCCACTCCTAATCTCT and the *Pck1p*-luc reverse primer CCGGAATGCCAAGCTCAGAGATCGCTGAGCGCCT. We generated a pcDNA3.1 Foxk1-Flag mutant by removing 40 amino acids from the N-terminal using the Foxk140Δ forward primer GCGCAACCTCCACCCGGG and the Foxk140Δ reverse primer TTCGGCCATGGTGGCGGATC, and a Q5 Site-Directed Mutagenesis Kit (New England BioLabs). pRL2-3xIRS has been described (17). HEK293 cells ($0.5–1 \times 10^6$) were seeded in each well of a 12-well plate. DNA (200 ng of pGL3-Pck1p, pGL3-G6pcp, Foxk1-Flag, or Foxk140del, or FoxO1, or red fluorescent protein [control]) and 20 ng of pRL-CMV plasmids were mixed with Lipofectamine 3000 transfection reagents in 0.1 mL Opti-MEM medium (Thermo Fisher Scientific) and added to each well after being incubated at room temperature for 15 min. After 36 h, we aspirated the culture medium, washed cells once with PBS, and lysed them in 0.35 mL lysis buffer. We performed luciferase assays using the Dual-Luciferase Reporter Assay System (Promega). The signals were read and recorded with an Orion L microplate luminometer. Plasmids are available upon request.

Chromatin Immunoprecipitation

We used a ChIP-IT High Sensitivity kit (Active Motif, Carlsbad, CA) for chromatin immunoprecipitation (ChIP) assay following the manufacturer's protocol. We sonicated 300 mg of liver using an S220 Focused-ultrasonicator (Covaris) to obtain sheared chromatin. Immunoprecipitation was performed using 4 μg of anti-FOXK1 antibody (Abcam, Cambridge, MA) for 10 μg of sheared chromatin. Real-time ChIP–qPCR were carried out using GoTaq qPCR Master Mix (Promega). The signals of binding events were normalized against input DNA for primer efficiency according to the protocol of a ChIP-IT qPCR Analysis Kit (Active Motif). Negative primers for qPCR analysis were purchased from Active Motif. Primers used to detect FOXK1 binding sites on *G6pc* or *Pck1* promoters are listed in Supplementary Table 9.

Immunohistochemistry

Mice (8- to 12-weeks old) were deprived of food overnight, and a subset was allowed to refeed for 1 h. We killed the mice, collected liver tissue, and fixed it in 4% paraformaldehyde for 2 h. We rinsed the tissue in PBS and then transferred it to 30% sucrose for dehydration overnight at 4°C, after which we embedded it in OCT compound (Sakura, Torrance, CA) and froze it at –80°C. Tissue blocks were sectioned into 8-μm-thick slices, which were rinsed with PBS three times and incubated in HistoVT One buffer (Nacalai USA, San Diego, CA) at 70°C for 30 min. After being blocked with 10% donkey serum in PBST (1X PBS supplemented with 0.1% Triton X-100) at room temperature for 30 min, tissue sections were incubated with FoxK1 antibody (1:500) at room temperature for 2 h and then with Alexa 488 donkey antirabbit antibody (1:400; Thermo Fisher Scientific) for 1 h. Frozen sections were counterstained with Hoechst stain (1:1,000; Thermo Fisher Scientific) for 5 min. Slides were mounted with Dako Glycergel and imaged with an Olympus fluorescent microscope.

Statistical Analysis

Each experiment was replicated at least three times for each condition. The liver tissue underwent MS once. We used the two-tailed Student *t* test and one-way ANOVA for statistical analysis; $P < 0.05$ indicated statistical significance. All data are presented as the mean ± SEM.

RESULTS

Identification of Hormone-Regulated TFs Through DNA Pull Down and MS

To interrogate the functional diversity of hormone-regulated TFs, we leveraged the observation that hepatic *Pck1* and *G6pc* share transcriptional regulators such as GR, FoxO1, CREBP, and C/EBPs α and β (1). However, when we ablated FoxO1 in primary hepatocytes with >99% efficiency using adenovirus-Cre, *G6pc* induction by D/C and by D/C/I were abolished, whereas *Pck1* induction by D/C decreased by only ~50% (5,18) (Fig. 1*A–C*). The findings illustrate the functional diversity in the

hormonal regulation of these two genes, which we set out to explore.

To this end, we combined DNA affinity purification ("pull down") with MS. We prepared nuclear extracts from the liver or primary hepatocytes of mice that were deprived of food or refed; the liver or cells were treated with various combinations of D/C/I and then incubated with biotin-labeled PCR fragments encompassing the insulin-responsive promoters of *Pck1* (*Pck1p*) (19) or *G6pc* (*G6pcp*) (20). After affinity purification on streptavidin beads and gel electrophoresis, we performed nano liquid chromatography–MS to identify bound proteins (21) (Fig. 1*D* and Supplementary Fig. 1*A*). We ranked identified TFs using the iBAQ method (22). To determine hormone responsiveness, we established an arbitrary iBAQ ratio (>1.5 or <0.5) for use when comparing intact liver from refed mice with liver from mice deprived of food; we used D/C versus the vehicle and D/C/I versus D/C when comparing primary hepatocytes. We divided hormone-regulated TFs into those enriched by hormone treatment (iBAQ ratio >1.5) and those depleted by hormone treatment (iBAQ ratio <0.5). We excluded from the analysis TFs with iBAQ ratios >0.5 and <1.5. Further analyses determined common TFs found in both promoters in primary hepatocytes and in liver, as well as promoter-specific TFs (Fig. 1*E*). Finally, we performed functional studies of primary hepatocytes to validate FoxK1, a TF candidate that emerged from this stepwise analysis (Fig. 1*E*).

To test the method, we first used Western blotting to examine candidate TFs in cytoplasmic and nuclear extracts of primary hepatocytes. Consistent with the literature, we

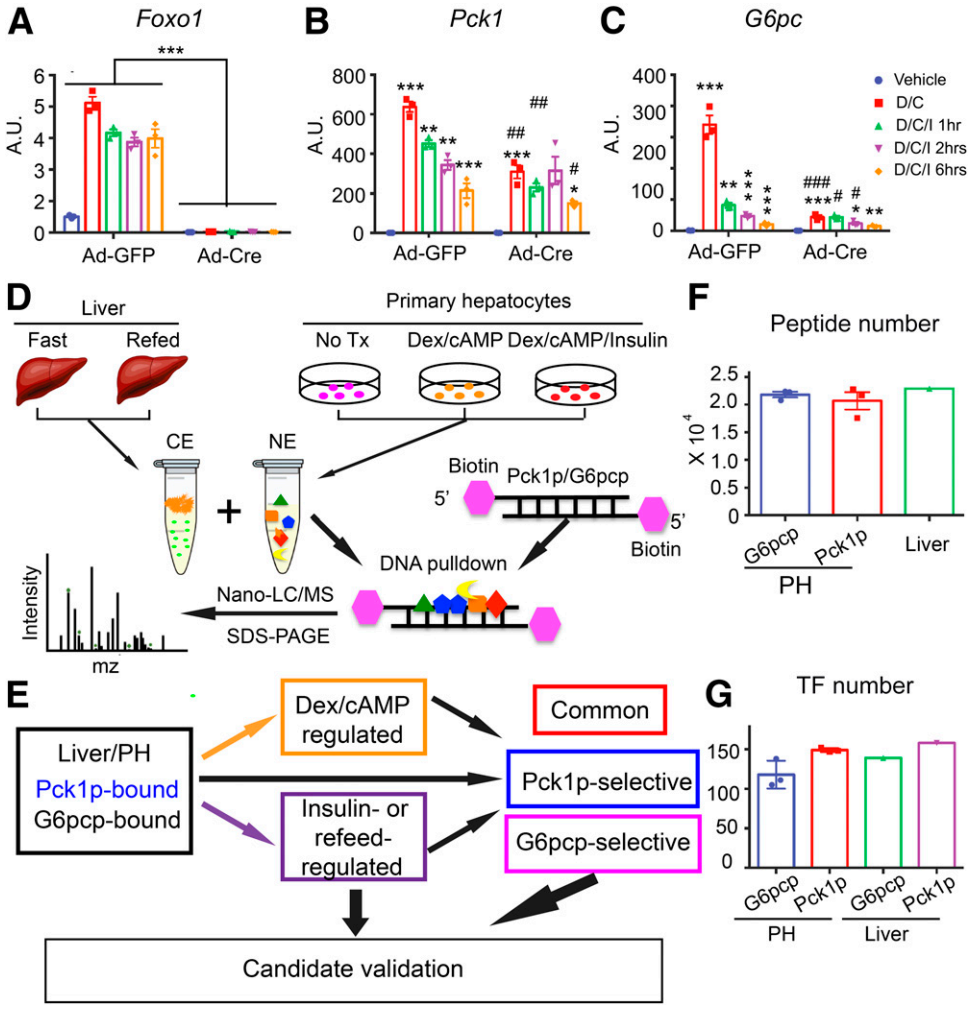

Figure 1—DNA pull down and MS analysis. *A–C*: qPCR analysis of *Foxo1* (*A*), *Pck1* (*B*), and *G6pc* (*C*) expression in primary hepatocytes treated with the vehicle, D/C, or D/C/I for the indicated amounts of time. Gene expression was normalized to cyclophilin A. *D*: Workflow for identifying hormone-regulated TFs by using DNA pull down and MS. *E*: Flowchart of analysis of TFs after they were identified by MS. *F* and *G*: The numbers of peptides (*F*) and TFs (*G*) identified in liver and primary hepatocytes. *Within-group comparison among different treatments. #Between-group comparison for the same treatment. Data are from three independent biological replicates. *,#$P < 0.05$; **,##$P < 0.01$; ***,###$P < 0.001$. Ad-Cre, adenovirus-Cre; Ad-GFP, adenovirus–green fluorescent protein; A.U., arbitrary units; CE, cytoplasmic extract; LC, liquid chromatography; NE, nuclear extract; No Tx, no treatment; PH, primary hepatocytes.

found that D/C treatment induced time-dependent nuclear entry of GR (23,24), whereas insulin promoted the nuclear exit of FoxO1 (25) (Supplementary Fig. 1*B*). Silver staining of polyacrylamide gels demonstrated enrichment of the initial material (Supplementary Fig. 2*A*). Accordingly, we detected FoxO1 and GR on Western blots of *Pck1p* pull-down samples (Supplementary Fig. 1*C*). These data indicate the feasibility of this method for use in identifying hormone-regulated TFs. The number of total and unique peptides identified was comparable between and reproducible in all MS determinations (Fig. 1*F*, Supplementary Fig. 2*C* and *D*, and Supplementary Table 1). TFs accounted for ~5% of all nuclear proteins identified, and 100–150 proteins were included in each MS experiment (Fig. 1*G*) in liver and in primary hepatocytes.

Feeding-Regulated *Pck1p* and *G6pcp* TFs in Liver

We first performed MS once with hepatic nuclear extracts from mice deprived of food and from refed mice. As a control, we showed that depriving mice of food promoted FoxO1 binding to *Pck1p* and *G6pcp*, whereas refeeding inhibited it, with a stronger effect on *G6pcp* than on *Pck1p* (Fig. 2*A*). Heat maps of TFs identified by MS showed extensive similarities between the two promoters (Fig. 2*B*). Indeed, we identified 128 common TFs for *G6pcp* and *Pck1p*, 30 TFs selective to *Pck1p*, and 11 selective to *G6pcp* (Fig. 2*C* and Supplementary Table 2). Analysis of TFs found on both promoters in the Kyoto Encyclopedia of Genes and Genomes highlighted pathways associated with metabolic diseases such as maturity-onset diabetes of the young, circadian rhythm, nonalcoholic fatty liver disease, hepatocellular carcinoma, and insulin resistance (Supplementary Table 6). Analysis of *Pck1p*-selective TFs in the Kyoto Encyclopedia of Genes and Genomes identified insulin resistance, transcriptional dysregulation in cancer, and cellular senescence as top functional pathways (Supplementary Table 2).

Next we determined which of these TFs were regulated by refeeding (Supplementary Table 2). Refeeding enriched 95 TFs on *G6pcp* and 92 on *Pck1p*; this accounts for 60% of the totals. Of these TFs, 63 were common between the two promoters. Refeeding depleted 15 TFs from *G6pcp* and 23 from *Pck1p* (Fig. 2*D*). Eight of these were common to both promoters. These data begin to explain differences in the responses of the two promoters to insulin: about one-third of refeeding-regulated TFs are selective to *G6pcp* or *Pck1p*. It is notable that refeeding results in an overall

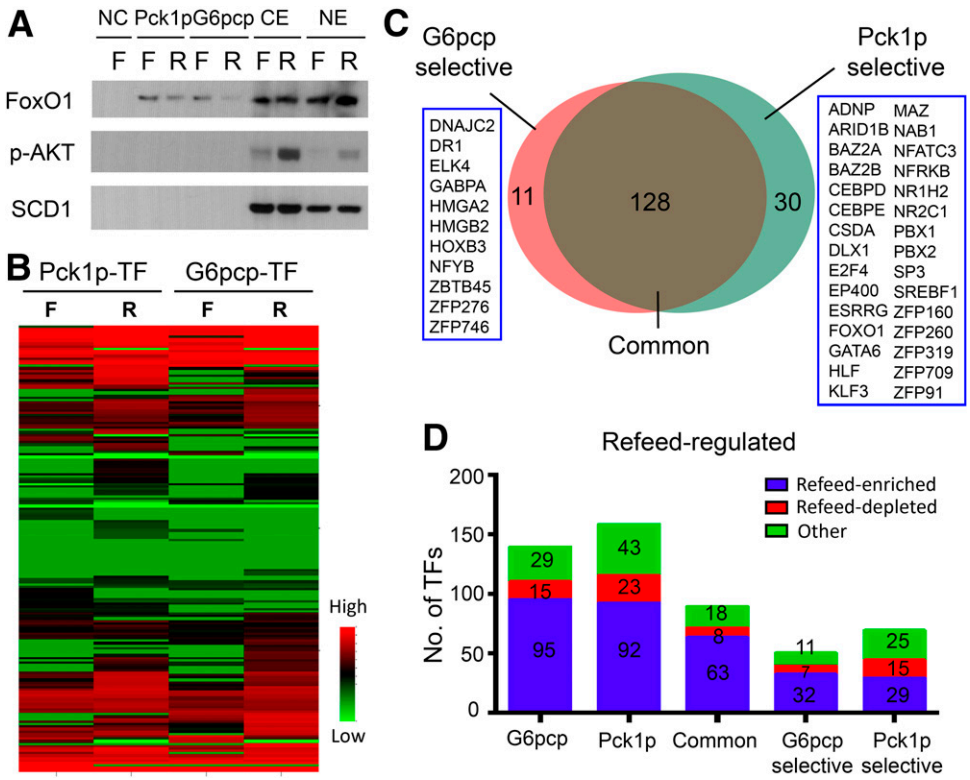

Figure 2—Identification of *G6pcp* and *Pck1p* TFs in liver. *A*: Detection of FoxO1 and phosphorylated Akt (p-AKT) in *Pck1p* and *G6pcp* pull down by Western blotting of the cytoplasmic extract (CE) and nuclear extract (NE) from mice deprived of food for 16 h (F) and mice that were refed (deprived of food for 16 h then refed over 4 h [R]). SCD1 was used as the loading control. *B*: Heat map of TFs identified from MS of *Pck1p* and *G6pcp* pull-down samples from the liver. *C*: The number of common and selective TFs identified on *G6pcp* and *Pck1p*, and a list of selective TFs for each promoter. All 128 common TFs are listed in Supplementary Table 2. *D*: The number of common and selective refeeding-regulated TFs on *G6pcp* and *Pck1p*. A complete list is available in Supplementary Table 2.

enrichment of TFs bound to the two promoters, consistent with active repression by insulin rather than—or in addition to—clearance of activators. In addition, LXRβ (NR1H2) and peroxisome proliferator–activated receptor α (PPARα) stand out as novel candidates among *Pck1p*-specific TFs; transcription factor 7-like 2 (TCF7L2), the premier genetic marker of susceptibility to diabetes, stands out as a shared TF (Supplementary Table 2).

Hormone-Responsive *Pck1p* and *G6pcp* TFs in Primary Hepatocytes

Next we performed similar experiments in primary hepatocytes in order to exclude the contributions from other cell types present in whole liver and to fine-tune the hormonal response by comparing three states: basal (no hormone), D/C (to represent a fasted state), and D/C/I (to represent a fed state) (Supplementary Fig. 2 and Supplementary Table 1). Western blotting of pull-down samples from primary hepatocytes demonstrated that D/C increased the binding of FoxO1 to *Pck1* and *G6pc*, whereas insulin decreased it, as expected (Fig. 3*A*). Heat maps of TF profiles identified in two separate experiments illustrate that TF decoration of *Pck1p* and *G6pcp* differs substantially (Fig. 3*B*). From three independent MS experiments performed for each promoter, we identified 79 common TFs on *G6pcp* and 82 on *Pck1p* (Fig. 3*C* and Supplementary Table 3). A total of 54 TFs were common to both promoters, 25 bound selectively to *G6pcp*, and 28 bound selectively to *Pck1p* (Fig. 3*C* and Supplementary Table 3). Pathway analysis of the 54 shared TFs identified three disease processes: maturity-onset diabetes of the young, hepatocellular carcinoma, and thermogenesis; this is consistent with the results of the liver study (Supplementary Table 3). Of the TFs shared between the two promoters, 46 were also among those TFs common to both promoters in the whole liver (Fig. 3*C* and Supplementary Table 3).

The number of TFs detected in each experiment and their regulation by D/C remained constant in the various experiments (Supplementary Fig. 3*A* and *B*). On average, ~40% of TFs (26 for *G6pcp* and 43 for *Pck1p*) were affected by D/C treatment (Supplementary Table 4). Six TFs became enriched at both promoters in response to D/C: ARID5B, CEBPB, NFIL3, MTA, NRF1, and SALL1 (Fig. 3*D* and Table 1). In contrast, JUNB and SMAD3 were the only two common TFs depleted by D/C treatment (Table 1).

Next we sorted *G6pcp* and *Pck1p* TFs on the basis of their response to insulin. The percentage of insulin-responsive TFs was constant at ~30% in each *G6pcp* experiment, whereas it varied more widely among *Pck1p* experiments (Supplementary Fig. 3*C* and *D*). We found 14 insulin-regulated TFs on *G6pcp* and 33 on *Pck1p*. Only two were common to both: BPTF and SMAD3; the others were promoter-specific (Table 1 and Fig. 3*E*). Liver and primary hepatocytes had 13 insulin-responsive TFs in common (Table 1 and Supplementary Table 2).

The insulin response sequence (IRS) on *Pck1p* (–416 to –402 bp from the transcription start site) mediates insulin inhibition of *Pck1* (19). To pare down the list of insulin-regulated TFs on *Pck1p*, we performed pull-down experiments using a *Pck1p*ΔIRS mutant (Supplementary Table 1). Whereas p-RNA Pol II bound equally to wild-type and ΔIRS mutant *Pck1p*, FoxO1 bound to wild-type *Pck1p* but not ΔIRS *Pck1p* (Fig. 3*F*); this is consistent with a critical role of this sequence in insulin's regulation of this promoter. Comparison of TFs detected by using wild-type and ΔIRS *Pck1p* identified 12 TFs that require an intact IRS to bind to *Pck1p* in an insulin-dependent manner (Fig. 3*G*, Table 1, and Supplementary Table 5). This list includes two forkhead proteins, FoxA2 and FoxK1.

In summary, MS pull down from liver and primary hepatocytes identified an array of *Pck1* and *G6pc* TFs, but only a fraction of them were hormone-responsive: in whole liver, ~60% were affected by refeeding; in primary hepatocytes, ~40% were affected by D/C and ~30%, by D/C/I. Interestingly, in intact liver the two promoters have in common the majority of TFs (~70%), whereas in primary hepatocytes the promoters share only 5–10% of the TFs. Nine insulin-responsive TFs are bound to *Pck1p* in both intact liver and primary hepatocytes, and four of them—FoxA2, FoxK1, ZFP91, and ZHX3—depend on an intact *Pck1p* IRS sequence for binding (Table 1).

Functional Characterization of FoxK1

The forkhead protein FoxK1 displayed features of an insulin-regulated *Pck1p* TF in primary hepatocytes and intact liver. Multiple analyses of DNA pull down and MS indicate that insulin increased its recruitment to *Pck1p* more than threefold in primary hepatocytes, and refeeding increased it approximately threefold in intact liver (Fig. 4*A*). Binding of FoxK1 required an intact *Pck1p* IRS (Table 1). FoxK1 is consistently associated with *Pck1p*, but we also detected it on *G6pcp* in a single experiment with primary hepatocytes (Fig. 4*B*). Western blotting of cytoplasmic and nuclear extracts from primary hepatocytes treated with D/C/I showed that insulin increased nuclear accumulation of FoxK1, depleting it from the cytoplasm (Fig. 4*C*). We detected an enrichment of FoxK1 in *Pck1p*, but not in *Pck1pΔIRS* pull-down samples, after they were treated with insulin (Fig. 4*D*). These findings confirm the MS data and indicate that insulin regulates the binding of FoxK1 to *Pck1p* through the IRS. A *3xIRS* luciferase assay revealed that both FoxK1 and FoxO1 bind to IRS and increase luciferase activity (Supplementary Fig. 4). Interestingly, when cotransfected with FoxO1, FoxK1 dose-dependently inhibited FoxO1's activity. The effect was abrogated by deleting the 40-amino-acid SIN3-interacting domain at the N-terminal end of FoxK1 (Supplementary Fig. 4). These data suggest that FoxK1 competes with FoxO1 to bind to the IRS and that the N-terminal domain is required for FoxK1's repressor function. Furthermore, the effect of insulin on FoxK1 was not due to increased transcription (at least in vitro), as *Foxk1*

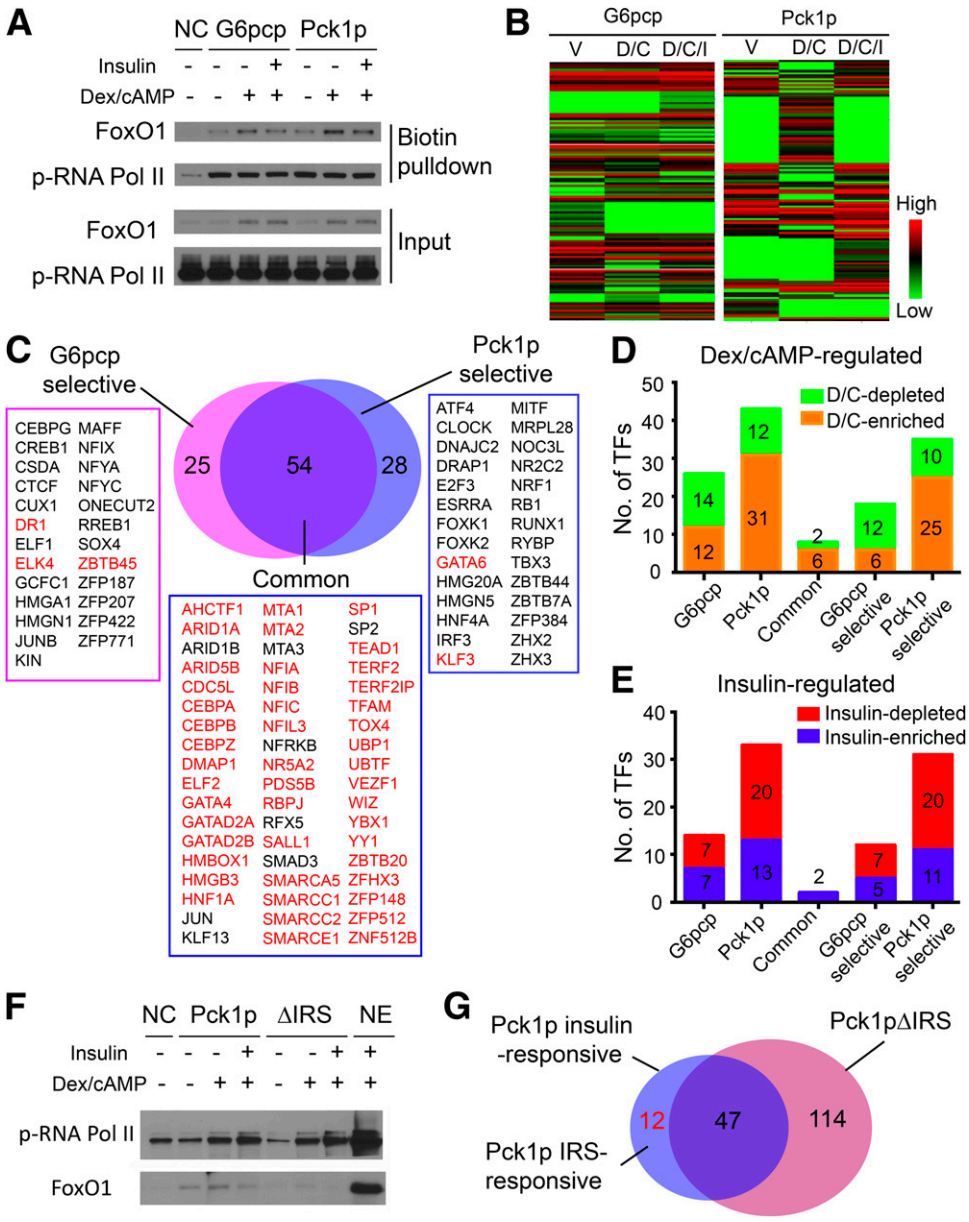

Figure 3—Identification of *G6pcp* and *Pck1p* TFs in primary hepatocytes. *A*: Western blots of FoxO1 and p-RNA pol II in *Pck1p* and *G6pcp* pull downs, created by using nuclear extracts from primary hepatocytes treated with D/C and D/C/I. *B*: Heat maps of TFs after hierarchical clustering from a representative *G6pcp* and *Pck1p* pull-down experiment. *C*: The number of common and selective TFs on *G6pcp* and *Pck1p*. TFs that were present in previous liver MS experiments are red. See also Supplementary Table 3. *D* and *E*: The number of common and selective *G6pcp* and *Pck1p* TFs regulated by D/C (*D*) or insulin (*E*) in primary hepatocytes. See also Supplementary Tables 4 and 5. *F*: Western blots of nuclear proteins after *Pck1p* or *Pck1pΔIRS* pull down. *G*: Comparison of IRS-dependent and IRS-independent insulin-regulated TFs on *Pck1p*. See also Supplementary Table 5. NC, negative control; NE, nuclear extract; V, vehicle.

mRNA levels actually decreased by ~50% in primary hepatocytes treated with insulin (Fig. 4*E*).

To document the in vivo function of FoxK1, we performed Western blotting on proteins isolated from DNA pull-down experiments; we detected FoxK1 on both *Pck1p* and *G6pcp* in the livers of refed mice (Fig. 4*F*). Next we immunostained liver sections from mice deprived of food and refed mice. When mice were deprived of food, FoxK1 localized to both the nucleus and the cytoplasm, whereas refeeding induced its accumulation in the nucleus (Fig. 4*G*). To confirm further the binding of FoxK1 to the promoters of these genes, we conducted ChIP–qPCR on liver samples using the FoxK1 antibody. We found that refeeding or insulin greatly increased FoxK1 binding to the Pck1 promoter (−509 to −393 bp) and the G6pc promoter (−266 to −135 bp) (Fig. 4*H* and Supplementary Fig. 5). However, only insulin robustly promoted FoxK1 binding. Moreover, the Pck1 promoter luciferase assay revealed that FoxK1 inhibits *Pck1* transcription (Fig. 4*I*). Removing 40 amino acids from the N-terminus of FoxK1,

Table 1—Hormone-regulated *Pck1p* and *G6pcp* TFs in primary hepatocytes

Pck1p TFs				G6pcp TFs		Common TFs	
D/C-regulated		Insulin-regulated	IRS-dependent	D/C-regulated	Insulin-regulated	D/C-regulated	Insulin-regulated
ARID5B	ATF4	*ATF4*	BPTF	*ARID5B*	*BPTF*	*ARID5B*	*BPTF*
CEBPB	E2F3	***FOXA2***	FOXA2	*CEBPB*	*CTCF*	*CEBPB*	*SMAD3*
MTA1	JUNB	***FOXK1***	FOXK1	*NFIL3*	***HNF4A***	*NFIL3*	
NFIL3	NR2C2	*RB1*	MAFF	*MTA1*	***NFYA***	*MTA1*	
NRF1	NR2F2	*TCF20*	NFYC	*NRF1*	*NOC3L*	*NRF1*	
SALL1	ONECUT2	***TCF7L2***	NRF1	*SALL1*	*SMAD3*	*SALL1*	
AHCTF1	RUNX1	***ZFP91***	RB1	*ELK4*	***VEZF1***	JUNB	
ARID1A	SMAD3	***ZHX3***	RBPJ	*MAFF*	ELF1	SMAD3	
ARID1B	TBX3	***WIZ***	RYBP	*NFIA*	HMGA1		
CEBPZ	TCF7L2	*BPTF*	TBX3	*TEAD1*	HMGN1		
CSDE1	TCFAP4	***CLOCK***	ZFP91	*ZFHX3*	NFIA		
DMAP1	ZFP91	*KLF3*	ZHX3	*ZFP148*	ONECUT2		
DNAJC2		*SMAD3*		HMBOX1	TCF7L2		
ESRRA		ARID5B		ARID1B	**ZFP422**		
FOXK2		DMAP1		CSDA			
GATA6		DNAJC2		DRAP1			
GATAD2B		DRAP1		ELF2			
HMGN5		HMG20A		HNF4A			
KLF13		HMGN5		JUNB			
MITF		MITF		NOC3L			
MTA2		MRPL28		NR5A2			
MTA3		NFYC		RYBP			
NFYC		NRF1		SMAD3			
NOC3L		TBX3		SMARCC2			
TCFCP2L1		**TERF2**		ZBTB45			
TERF2		TFAM		ZFP187			
VEZF1		YY1					
ZBTB44		ZBTB20					
ZFP384		ZBTB44					
ZFP512		ZBTB45					
ZNF512B		ZBTB7A					
		ZFP384					
		ZFP512					

Hormone-enriched TFs are italicized, and hormone-depleted TFs are underlined. TFs also found in the liver of refed animals are set in boldface type.

corresponding to the SIN3-interacting domain, fully restored *Pck1* transcription. These data confirm that FoxK1 is an insulin-regulated TF in vivo and may function as a transcription repressor in controlling *Pck1* and *G6pc* expression.

FoxK1 Regulates Hepatocyte Glucose Production

The studies described above demonstrate that insulin and refeeding promote the binding of FoxK1 to *Pck1p* and *G6pcp*. Next we explored the role of FoxK1 in glucose production by primary hepatocytes. By transfecting two siRNAs, we reduced FoxK1 levels by ~80% (Fig. 5*A*). Glucose production assays showed that *FoxK1* knockdown not only blunted insulin's ability to suppress this process but also partly reduced its induction by D/C (Fig. 5*B*). It should be noted that some FoxK1 exists in the nuclei of D/C-treated cells. Accordingly, D/C failed to induce PCK1 and G6PC protein levels (Fig. 5*C*) and mRNA levels (Fig. 5*D* and *E*). Phosphorylated Akt levels did not change, indicating that the effect of FoxK1 is not due to increased insulin signaling; we did observe slight decreases of FoxO1 and PGC1α protein levels (Fig. 5*C*), which might contribute to the effects on G6PC and PCK1. qPCR analysis confirmed that FoxK1 knockdown impaired D/C-induced

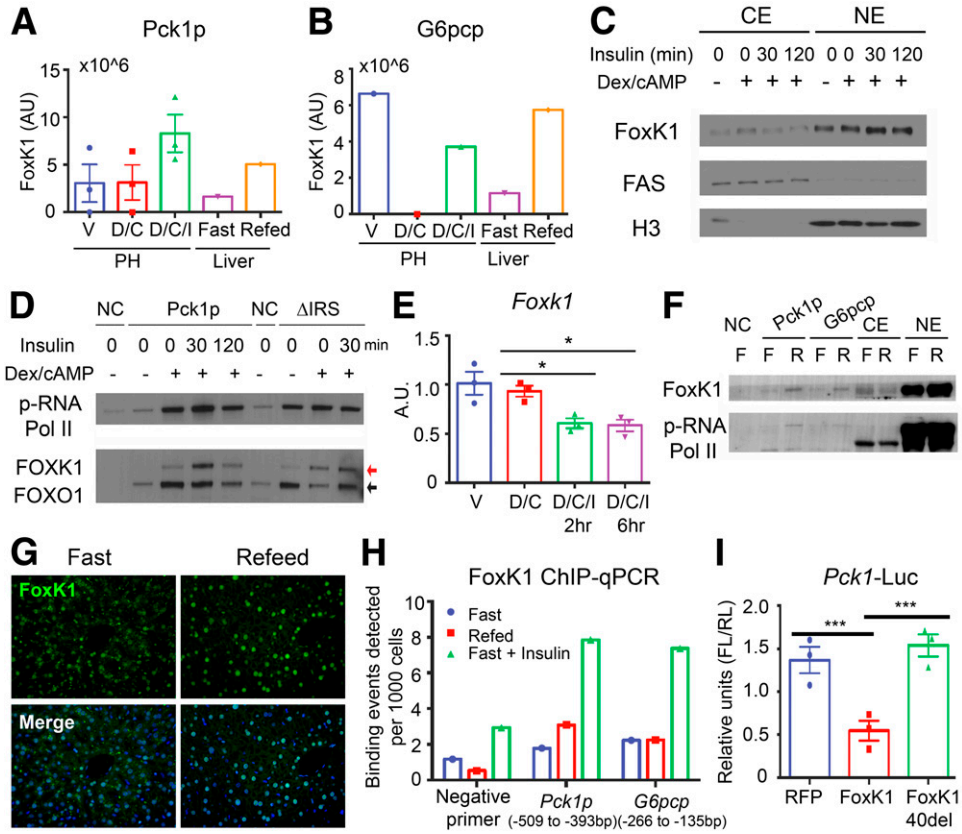

Figure 4—Insulin regulation of FoxK1. FoxK1 level in *Pck1p* ($n = 3$) (*A*) or *G6pcp* ($n = 1$) (*B*) pull down in primary hepatocytes (PH) and liver under different conditions, as identified from MS experiments. *C*: Western blots of FoxK1 in the cytoplasmic extract (CE) and nuclear extract (NE) from PH treated with the vehicle (V), D/C, and D/C/I. FAS and histone H3 were used as loading controls. *D*: Western blots of FoxK1, p-RNA Pol II, and FoxO1 in *Pck1p* and *Pck1pΔIRS* pull downs. *E*: *Foxk1* mRNA in PH treated with V, D/C, or D/C/I for the indicated amounts of time. *F*: FoxK1 immunostaining in livers of mice deprived of food for 16 h (F) and mice that were refed (deprived of food for 16 h then refed over 4 h [R]). Nuclei were stained with Hoechst stain. *G*: Western blotting of FoxK1 in liver DNA pull downs. p-RNA Pol II was used as the control. *H*: ChIP–qPCR analysis of FoxK1 binding sites on *Pck1* and *G6pc* promoters. Chromatin DNA was isolated from livers of mice deprived of food, mice that were refed, and mice that were deprived of food and treated with insulin (1 units/kg) for 15 min. The two promoter regions of *Pck1* and *G6pc* are indicated. *I*: In the *Pck1* promoter luciferase reporter assay, 293 cells were transfected with red fluorescent protein (RFP), FoxK1, or FoxK140Δ, together with luciferase constructs that contain the *Pck1* promoter. Cells were collected and analyzed 36 h after transfection. The Student *t* test was used for all analyses. Each bar represents the data from three independent biological replicates. $^{*}P < 0.05$; $^{***}P < 0.001$. 40del, N-terminal 40aa deletion; AU, arbitrary units; FL, firefly luciferase; NC, negative control; RL, Renilla luciferase.

Ppargc1a and *Fbp1* expression without affecting *Foxo1* or *Gck* (Fig. 5*D*–*I*). These data are consistent with a role of FoxK1 in the inhibition of glucose production by insulin and in integrating signals from counterregulatory hormones. The same siRNA sequences, expressed through an adenoviral vector, failed to lower FoxK1 levels in intact liver, preventing physiologic analysis. On the basis of our in vitro studies, however, we expect that FoxK1 ablation in mouse liver will reduce hepatic glucose production and improve glucose tolerance. Conditional knockout animals are being generated and related data will be reported in subsequent publications.

DISCUSSION

In this study we used MS of peptides isolated by biotin-labeled DNA affinity purification to identify a diverse group of TFs that bind to the proximal *Pck1* and *G6pc* promoters in a hormone-regulated manner. We identified three general and seemingly novel features of this analysis: *1*) The repertoire of hormone-regulated TFs is unexpectedly diverse. *2*) The patterns in which TF binds to the two test promoters overlap more in intact liver than in primary hepatocytes; in the latter, *Pck1* and *G6pc* seem to be regulated through largely divergent TFs. *3*) Insulin treatment preferentially results in increased occupancy by the two promoters, consistent with a model in which the hormone's primary role is to recruit corepressors rather than to clear activators. This is consistent with the function of FoxK1 (see below) and highlights the unique role of FoxK1 in insulin's actions on *Pck1* and *G6pc*.

Methodological Limitations

This approach has obvious limitations: *1*) It can analyze only short sequences and cannot account for enhancers or long-range interactions. *2*) It is intrinsically sensitive to the stability of DNA-protein and protein-protein interactions. *3*) Because the target DNA is present in excess, the method may overestimate the actual number of TFs binding to endogenous

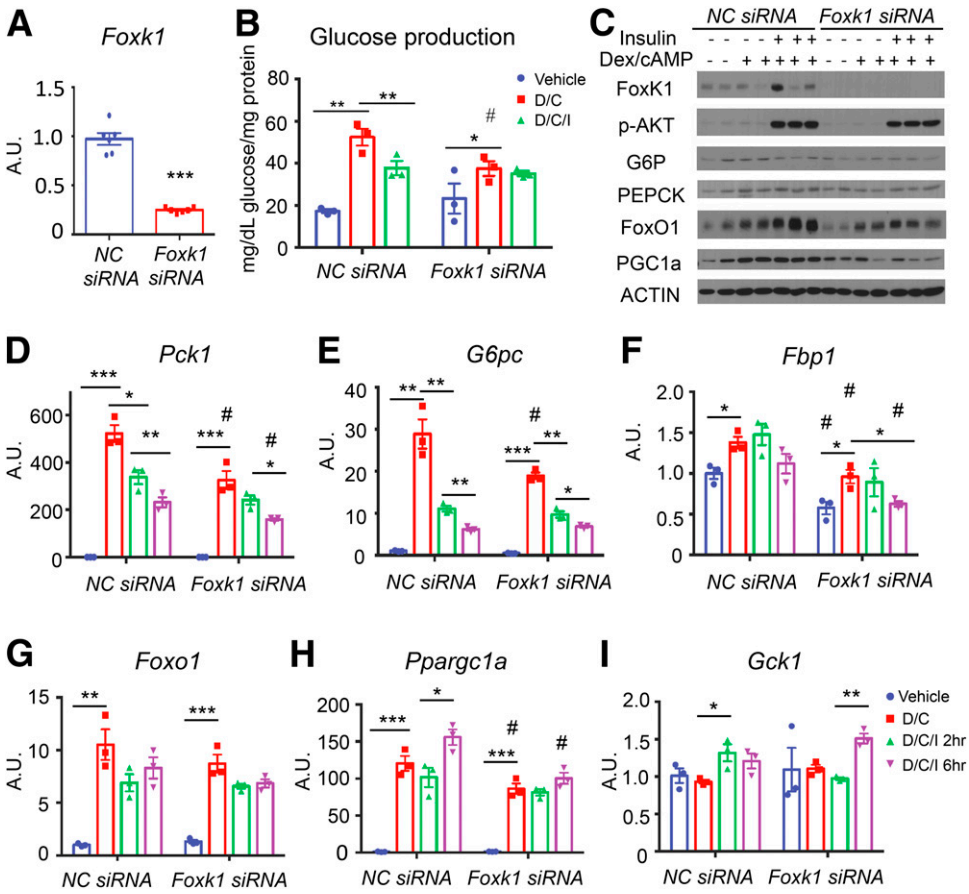

Figure 5—*Foxk1* knockdown reduces glucose production by hepatocytes. *A*: *Foxk1* knockdown in primary hepatocytes using siRNA ($n = 6$ for each bar). *B*: Glucose production in primary hepatocytes after siRNA transfection. *C*: Western blots of primary hepatocyte extracts under various conditions after siRNA transfection. *D–I*: qPCR analysis of *Pck1* (*D*), *G6pc* (*E*), *Fbp1* (*F*), *Foxo1* (*G*), *Ppargc1a* (*H*), and *Gck1* (*I*) in siRNA-transfected primary hepatocytes treated with various hormones. The Student *t* test was used for all analyses. Each bar represents the data from three independent biological replicates. *Within-group comparison. #Between-group comparison for the same treatment. *,#$P < 0.05$; **$P < 0.01$; ***$P < 0.001$. A.U., arbitrary units; NC, negative control.

target promoters; this may explain experimental variations in the detection of TFs. For example, we readily detected FoxO1 through Western blotting of *Pck1p* and *G6pcp* pull-down samples, but its detection by MS varied. However, because this feature dovetails with FoxO1 regulation of Pck1 (i.e., it is variable), it strengthens the relevance of these results. With regard to G6pc, the failure of MS to detect FoxO1 can be explained by the presence of genomic sites that are alternatives to those included in our pull-down assays, or by the time course of FoxO1 binding to *G6pcp*. The variability of the various experiments may also be related to hepatocyte heterogeneity, sensitivity to the treatment steps, abundance of the target protein, or interactions between hepatocytes and other cells such as stellate, Kupffer, and endothelial cells. Systematic functional characterization of the newly identified candidate TFs will address lingering questions.

FoxK1 in Hormone-Regulated Glucose Metabolism

A novel finding of this work is the identification of FoxK1 as an insulin-regulated TF with a role in glucose production by hepatocytes. Among forkhead TFs, FoxK1 is thought to function as a repressor with roles in myogenic differentiation, cell proliferation, and autophagy (26–29). It has been shown to be phosphorylated by mTORC1, promoting its nuclear exclusion (30), and it has been loosely associated with glucose metabolism in liver tumor cell studies (31). To our knowledge, its involvement in insulin action has not been previously disclosed. Interestingly, it seems to act as an insulin-recruited repressor of gene expression. In this regard, it possesses a Sin3A-interaction domain at the N-terminus that is important to its repressor function, possibly by recruiting Sin3a to target promoters, similar to the mechansim of action of FoxO1 (15). In vivo studies to address this question will have to take into account a second isoform, FoxK2, with potentially similar functions (26,32).

New TF Candidates and Therapeutic Targets for Type 2 Diabetes

Our study identified almost all TFs previously associated with the regulation of hepatic glucose metabolism by insulin, such as HNF4α, C/EBPβ, LXRβ, FoxA2, and RBPj (11,18,33,34). This finding increases our confidence that newly identified TFs represent physiologic mediators

of hormone signaling, some of which may provide alternative targets of treatment to reduce hepatic glucose production in type 2 diabetes.

LXRβ and PPARα stand out as novel candidates among *Pck1p*-specific TFs. Given the resurgence of interest in ligands of these nuclear receptors, it is important to keep in mind that our studies suggest that they are specific to *Pck1p* and that they bind to *Pck1p* during food deprivation and are depleted upon refeeding. Therefore, antagonists, rather than agonists, may be useful in reducing hepatic glucose production (35,36).

An important new finding of this work is the identification of TCF7L2 as an insulin-regulated *Pck1* TF. TCF7L2 is contained within the main type 2 diabetes susceptibility locus identified in multiple genome-wide association studies of different ethnic groups (37,38). Although TCF7L2 had been suggested to affect primarily pancreatic β-cell function (39–41), evidence is not definitive (42). The identification of TCF7L2 as an insulin-regulated TF on *Pck1p* in primary hepatocytes and liver is consistent with its role in glucose production and provides a new testable hypothesis of the mechanism of diabetes susceptibility linked to this locus.

We found 14 insulin-regulated TFs on *G6pcp* and 33 on *Pck1p*. Only two were common to both: BPTF and SMAD3. SMAD3 lies in the transforming growth factor-β pathway and has been implicated in the development of liver fibrosis (43,44). Evidence linking it to hepatic gluconeogenesis through protein phosphatase 2A, AMPK, and FoxO1 is limited (45). Our study indicates that SMAD3 is depleted by D/C and enriched by insulin on *Pck1* and *G6pc*, consistent with a role in suppressing these genes. The TFs newly identified in this study provide candidates that might deconvolute the regulation of hepatic glucose production and may be potential targets for diabetes treatment.

NOTE ADDED IN PROOF

While this paper was under review, two additional articles describing a metabolic role of Foxk1 (and Foxk2) appeared: Sakaguchi M, Cai W, Wang CH, et al. FoxK1 and FoxK2 in insulin regulation of cellular and mitochondrial metabolism. Nat Commun 2019;10:1582; and Sukonina V, Ma H, Zhang W, et al. FOXK1 and FOXK2 regulate aerobic glycolysis. Nature 2019;566:279–283.

Acknowledgments. The authors thank KyeongJin Kim and Junjie Yu, Columbia University Medical Center, for helpful discussions.

Funding. This work was supported by New York Obesity Research Center Training Grant T32-DK755925 (to L.W.) and through National Institutes of Health and National Institute of Diabetes and Digestive and Kidney Diseases grants DK57539 (to D.A.) and DK63618 (to the Columbia Diabetes Research Center).

Duality of Interest. No potential conflicts of interest relevant to this article were reported.

Author Contributions. L.W. designed and performed all experiments and wrote the manuscript. Q.L. and J.H. analyzed the mass spectrometry data. T.K. performed the ChIP-qPCR experiment. J.Q. and D.A. conceived the experimental design, analyzed and discussed the data, and wrote the manuscript. D.A. is the guarantor of this work and, as such, had full access to all the data in the study and takes responsibility for the integrity of the data and the accuracy of the data analysis.

Data Availability. The data supporting the findings of this study are available within the article and the Supplementary Data, or they are available upon reasonable request to the authors. The research resources mentioned in this study are also available upon request.

References

1. Lin HV, Accili D. Hormonal regulation of hepatic glucose production in health and disease. Cell Metab 2011;14:9–19
2. Bergman RN, Iyer MS. Indirect regulation of endogenous glucose production by insulin: the single gateway hypothesis revisited. Diabetes 2017;66:1742–1747
3. Horton JD, Bashmakov Y, Shimomura I, Shimano H. Regulation of sterol regulatory element binding proteins in livers of fasted and refed mice. Proc Natl Acad Sci U S A 1998;95:5987–5992
4. Herzig S, Long F, Jhala US, et al. CREB regulates hepatic gluconeogenesis through the coactivator PGC-1. Nature 2001;413:179–183
5. Matsumoto M, Pocai A, Rossetti L, Depinho RA, Accili D. Impaired regulation of hepatic glucose production in mice lacking the forkhead transcription factor Foxo1 in liver. Cell Metab 2007;6:208–216
6. Liang G, Yang J, Horton JD, Hammer RE, Goldstein JL, Brown MS. Diminished hepatic response to fasting/refeeding and liver X receptor agonists in mice with selective deficiency of sterol regulatory element-binding protein-1c. J Biol Chem 2002;277:9520–9528
7. Haeusler RA, Hartil K, Vaitheesvaran B, et al. Integrated control of hepatic lipogenesis versus glucose production requires FoxO transcription factors. Nat Commun 2014;5:5190
8. Lee D, Le Lay J, Kaestner KH. The transcription factor CREB has no non-redundant functions in hepatic glucose metabolism in mice. Diabetologia 2014;57:1242–1248
9. Dentin R, Liu Y, Koo SH, et al. Insulin modulates gluconeogenesis by inhibition of the coactivator TORC2. Nature 2007;449:366–369
10. Imai E, Miner JN, Mitchell JA, Yamamoto KR, Granner DK. Glucocorticoid receptor-cAMP response element-binding protein interaction and the response of the phosphoenolpyruvate carboxykinase gene to glucocorticoids. J Biol Chem 1993;268:5353–5356
11. Liu S, Croniger C, Arizmendi C, et al. Hypoglycemia and impaired hepatic glucose production in mice with a deletion of the C/EBPbeta gene. J Clin Invest 1999;103:207–213
12. Roesler WJ, Crosson SM, Vinson C, McFie PJ. The alpha-isoform of the CCAAT/enhancer-binding protein is required for mediating cAMP responsiveness of the phosphoenolpyruvate carboxykinase promoter in hepatoma cells. J Biol Chem 1996;271:8068–8074
13. Haeusler RA, Kaestner KH, Accili D. FoxOs function synergistically to promote glucose production. J Biol Chem 2010;285:35245–35248
14. Liu Q, Ding C, Liu W, et al. In-depth proteomic characterization of endogenous nuclear receptors in mouse liver. Mol Cell Proteomics 2013;12:473–484
15. Langlet F, Haeusler RA, Linden D, et al. Selective inhibition of FOXO1 activator/repressor balance modulates hepatic glucose handling. Cell 2017;171:824–835.e18
16. Kummerfeld SK, Teichmann SA. DBD: a transcription factor prediction database. Nucleic Acids Res 2006;34:D74–D81
17. Tang ED, Nuñez G, Barr FG, Guan KL. Negative regulation of the forkhead transcription factor FKHR by Akt. J Biol Chem 1999;274:16741–16746
18. Pajvani UB, Shawber CJ, Samuel VT, et al. Inhibition of Notch signaling ameliorates insulin resistance in a FoxO1-dependent manner. Nat Med 2011;17:961–967
19. O'Brien RM, Lucas PC, Forest CD, Magnuson MA, Granner DK. Identification of a sequence in the PEPCK gene that mediates a negative effect of insulin on transcription. Science 1990;249:533–537
20. Schmoll D, Walker KS, Alessi DR, et al. Regulation of glucose-6-phosphatase gene expression by protein kinase Balpha and the forkhead transcription factor

FKHR. Evidence for insulin response unit-dependent and -independent effects of insulin on promoter activity. J Biol Chem 2000;275:36324–36333
21. Ding C, Jiang J, Wei J, et al. A fast workflow for identification and quantification of proteomes. Mol Cell Proteomics 2013;12:2370–2380
22. Schwanhäusser B, Busse D, Li N, et al. Corrigendum: global quantification of mammalian gene expression control. Nature 2013;495:126–127
23. Htun H, Barsony J, Renyi I, Gould DL, Hager GL. Visualization of glucocorticoid receptor translocation and intranuclear organization in living cells with a green fluorescent protein chimera. Proc Natl Acad Sci U S A 1996;93:4845–4850
24. Winkler R, Benz V, Clemenz M, et al. Histone deacetylase 6 (HDAC6) is an essential modifier of glucocorticoid-induced hepatic gluconeogenesis. Diabetes 2012;61:513–523
25. Nakae J, Barr V, Accili D. Differential regulation of gene expression by insulin and IGF-1 receptors correlates with phosphorylation of a single amino acid residue in the forkhead transcription factor FKHR. EMBO J 2000;19:989–996
26. Bowman CJ, Ayer DE, Dynlacht BD. Foxk proteins repress the initiation of starvation-induced atrophy and autophagy programs. Nat Cell Biol 2014;16:1202–1214
27. Meeson AP, Shi X, Alexander MS, et al. Sox15 and Fhl3 transcriptionally coactivate Foxk1 and regulate myogenic progenitor cells. EMBO J 2007;26:1902–1912
28. Shi X, Bowlin KM, Garry DJ. Fhl2 interacts with Foxk1 and corepresses Foxo4 activity in myogenic progenitors. Stem Cells 2010;28:462–469
29. Shi X, Wallis AM, Gerard RD, et al. Foxk1 promotes cell proliferation and represses myogenic differentiation by regulating Foxo4 and Mef2. J Cell Sci 2012;125:5329–5337
30. He L, Gomes AP, Wang X, et al. mTORC1 promotes metabolic reprogramming by the suppression of GSK3-dependent Foxk1 phosphorylation. Mol Cell 2018;70:949–960.e4
31. Cui H, Gao Q, Zhang L, Han F, Wang L. Knockdown of FOXK1 suppresses liver cancer cell viability by inhibiting glycolysis. Life Sci 2018;213:66–73
32. Shi X, Garry DJ. Sin3 interacts with Foxk1 and regulates myogenic progenitors. Mol Cell Biochem 2012;366:251–258
33. Wolfrum C, Asilmaz E, Luca E, Friedman JM, Stoffel M. Foxa2 regulates lipid metabolism and ketogenesis in the liver during fasting and in diabetes. Nature 2004;432:1027–1032
34. Zhang L, Rubins NE, Ahima RS, Greenbaum LE, Kaestner KH. Foxa2 integrates the transcriptional response of the hepatocyte to fasting. Cell Metab 2005;2:141–148
35. Komati R, Spadoni D, Zheng S, Sridhar J, Riley KE, Wang G. Ligands of therapeutic utility for the liver X receptors. Molecules 2017;22. pii: E88
36. Rigano D, Sirignano C, Taglialatela-Scafati O. The potential of natural products for targeting PPARα. Acta Pharm Sin B 2017;7:427–438
37. Grant SF, Thorleifsson G, Reynisdottir I, et al. Variant of transcription factor 7-like 2 (TCF7L2) gene confers risk of type 2 diabetes. Nat Genet 2006;38:320–323
38. Steinthorsdottir V, Thorleifsson G, Sulem P, et al. Identification of low-frequency and rare sequence variants associated with elevated or reduced risk of type 2 diabetes. Nat Genet 2014;46:294–298
39. Liu Z, Habener JF. Glucagon-like peptide-1 activation of TCF7L2-dependent Wnt signaling enhances pancreatic beta cell proliferation. J Biol Chem 2008;283:8723–8735
40. Loder MK, da Silva Xavier G, McDonald A, Rutter GA. TCF7L2 controls insulin gene expression and insulin secretion in mature pancreatic beta-cells. Biochem Soc Trans 2008;36:357–359
41. Takamoto I, Kubota N, Nakaya K, et al. TCF7L2 in mouse pancreatic beta cells plays a crucial role in glucose homeostasis by regulating beta cell mass. Diabetologia 2014;57:542–553
42. Accili D. Insulin action research and the future of diabetes treatment: the 2017 Banting Medal for Scientific Achievement lecture. Diabetes 2018;67:1701–1709
43. Lee JI, Wright JH, Johnson MM, et al. Role of Smad3 in platelet-derived growth factor-C-induced liver fibrosis. Am J Physiol Cell Physiol 2016;310:C436–C445
44. Xu F, Liu C, Zhou D, Zhang L. TGF-β/SMAD pathway and its regulation in hepatic fibrosis. J Histochem Cytochem 2016;64:157–167
45. Yadav H, Devalaraja S, Chung ST, Rane SG. TGF-β1/Smad3 pathway targets PP2A-AMPK-FoxO1 signaling to regulate hepatic gluconeogenesis. J Biol Chem 2017;292:3420–3432